THE JOURNAL OF BIOLOGICAL CHEMISTRY
Vol. 277, No. 38, Issue of September 20, pp. 35219–35224, 2002

Printed in U.S.A.

Identification of a Novel Na^+/*myo*-Inositol Cotransporter*

Received for publication, May 2, 2002, and in revised form, July 19, 2002
Published, JBC Papers in Press, July 19, 2002, DOI 10.1074/jbc.M204321200

Michael J. Coady‡, Bernadette Wallendorff, Dominique G. Gagnon, and Jean-Yves Lapointe

From the Groupe de Recherche en Transport Membranaire, Université de Montréal, Montréal, Quebec H3T 1J4, Canada

rkST1, an orphan cDNA of the SLC5 family (43% identical in sequence to the sodium *myo*-inositol cotransporter SMIT), was expressed in *Xenopus laevis* oocytes that were subsequently voltage-clamped and exposed to likely substrates. Whereas superfusion with glucose and other sugars produced a small inward current, the largest current was observed with *myo*-inositol. The expressed protein, which we have named SMIT2, cotransports *myo*-inositol with a K_m of 120 μM and displays a current-voltage relationship similar to that seen with SMIT (now called SMIT1). The transport is Na^+-dependent, with a K_m of 13 mM. SMIT2 exhibits phlorizin-inhibitable presteady-state currents and substrate-independent "Na^+ leak" currents similar to those of related cotransporters. The steady-state cotransport current is also phlorizin-inhibitable with a K_i of 76 μM. SMIT2 exhibits stereospecific cotransport of both D-glucose and D-xylose but does not transport fucose. In addition, SMIT2 (but not SMIT1) transports D-*chiro*-inositol. Based on previous publications, the tissue distribution of SMIT2 is different from that of SMIT1, and the existence of this second cotransporter may explain much of the heterogeneity that has been reported for inositol transport.

The first members of the vertebrate cotransporter protein family SLC5, which includes the high affinity Na^+/glucose cotransporter (SGLT1) and the Na^+/*myo*-inositol cotransporter (SMIT), were isolated over a decade ago based on expression of the proteins in *Xenopus laevis* oocytes (1, 2). Although substrates as diverse as proline, iodide, and vitamins (3) are transported by this family of proteins, the best characterized transporters remain SGLT1 and SMIT. There are also several "orphan" transporters whose cDNA has been cloned either by using labeled cDNA from members of the SLC5 family as biochemical probes or by comparing SLC5 sequence information *in silico* to data stored in DNA data bases (3); the newly discovered sequences are orphans in that they have no known function. Some of the orphan protein sequences are particularly similar to the protein sequences for SGLT1 and SMIT (4, 5) and presumably transport substrates similar or identical to either glucose or its isomer *myo*-inositol. The SLC5 proteins with known functions have generally been studied by voltage-clamp experiments because these proteins are electrogenic. Also, presteady-state currents are associated with expression of these proteins at the cell surface, and some (but not all, *e.g.* xSGLT1L (6)) SLC5 proteins also exhibit a substrate-independent Na^+ current ("Na^+ leak").

myo-Inositol (MI)[1] is the most biologically abundant stereoisomer of the inositols, cyclic polyols which serve as precursors to molecules involved in several important aspects of cell physiology, including cell signaling via the inositol phosphate pathways (7) and the production of phospholipids involved in cell adhesion and vesicular trafficking (8). MI also serves as a "compatible osmolyte" used to control intracellular osmolarity in various tissues, including kidney, brain, and endothelium (9–11). Although mammalian serum levels of MI are normally between 30 and 70 μM (12–14), the MI levels within mammalian cells can attain 30 mM (15). There appear to be several transport mechanisms involved in the active uptake of MI into various types of cells (16–19), and examples of tissues seeming to lack active transport of MI have also been described (20–22). In particular, one transporter that exhibits similar affinities for MI and for its epimer D-*chiro*-inositol has been demonstrated in the hepatic cell culture line HepG2 (18); in contrast, transport of D-*chiro*-inositol is not observed with the SMIT transporter (18). The proteins known to transport MI in mammals are SMIT and HMIT, a H^+/MI cotransporter from a completely different protein family (23).

In this work, we have found that a novel Na^+/MI cotransport activity is associated with expression of one of the orphan proteins of the SLC5 family (rkST1) (4) in *Xenopus* oocytes. The substrate specificities and transport kinetics of this protein exhibit both functional similarities to the previously cloned SMIT transporter as well as obvious differences, including the transport of D-*chiro*-inositol. The existence of this second cotransporter may explain some of the heterogeneity that has been reported for Na^+/MI uptake.

EXPERIMENTAL PROCEDURES

Materials—Unless otherwise noted, all of the chemicals were purchased from Sigma-Aldrich. D-glucose, D-xylose, and L-xylose were analyzed by high pressure liquid chromatography (courtesy of Douglas Heimark, Insmed Inc., Glen Allen, VA); none of the three sugars contained detectable levels of MI (>0.1%). D-*chiro*-Inositol and L-*chiro*-inositol were from Industrial Research Ltd. (Lower Hutt, New Zealand). Phlorizin was diluted at least 1:1000 from a 500 mM solution in ethanol. For studies where the concentration of phlorizin was varied, phlorizin crystals were dissolved directly into the saline solution.

DNA and RNA Preparation—The coding region of the rabbit cDNA rkST1 (4) was obtained by PCR on renal cDNA using the phosphorylated oligonucleotides GATCTCACCATGGAGAGCAGCACCAGCA and CTAGTCTAGGCGAAGTAGCCCCAGAGGAA (AlphaDNA, Montreal, Canada) and *Pfu* DNA polymerase (Stratagene, San Diego, CA). The ends of the PCR product were digested with Exonuclease III to yield 5′ overhangs (24). Following this, the DNA product was ligated between the *Bgl*II and *Spe*I sites of pT7T3, a vector designed for strong expression of transcripts in oocytes (kindly provided by Dr. Paul Krieg, University of Texas at Austin). Following purification of the recombinant plasmid, an aliquot of the DNA was cleaved by digestion with *Eco*RI, followed by *in vitro* transcription using T7 RNA polymerase (25).

* The costs of publication of this article were defrayed in part by the payment of page charges. This article must therefore be hereby marked "*advertisement*" in accordance with 18 U.S.C. Section 1734 solely to indicate this fact.

‡ To whom correspondence should be addressed: Groupe de Recherche en Transport Membranaire, P.O. Box 6128 succ. "Centre-Ville" Montréal, PQ H3C 3J7, Canada. Tel.: 514-343-6111 (ext. 3289); Fax: 514-343-7146; E-mail: coady@magellan.umontreal.ca.

[1] The abbreviations used are: MI, *myo*-inositol; I-V, current-voltage.

The identity of the cloned PCR product was confirmed by dideoxy sequencing. There were 8 base pairs that differed from the published rabbit rsKT1 cDNA sequence, resulting in one conservative alteration in the protein sequence (T173A)*.

Oocyte Preparation—The oocytes were removed from gravid female *X. laevis* frogs (Connecticut Valley Biological Supply Co., Southampton, MA) under tricaine anesthesia. The individually dissected oocytes were placed into a Ca^{2+}-free buffered saline solution (200 millosmolar) and defolliculated by collagenase digestion. The oocytes were maintained at 18 °C in Barth's solution (90 mM NaCl, 3 mM KCl, 0.82 mM $MgSO_4$, 0.41 mM $CaCl_2$, 0.33 mM $Ca(NO_3)_2$, 5 mM HEPES, pH 7.6) supplemented with 5% horse serum (26) (except where described), 2.5 mM sodium pyruvate, 100 units/ml penicillin, and 0.1 mg/ml streptomycin. RNA (46 nl, 0.1 μg/μl unless otherwise noted) was injected into the oocytes 1 day after surgical isolation; the oocytes were assayed for transporter activity at 5–8 days after the injection.

Steady-state Current Measurements—The oocyte currents were measured with a standard two-microelectrode voltage clamp technique as described previously (27). In brief, a commercial amplifier (oocyte clamp model OC-725, Warner Instruments, Hamden, CT) and a data acquisition system (RC Electronics, Santa Barbara, CA) were used to send voltage pulses to the oocyte as well as to simultaneously record membrane current and voltage signals. The oocyte was superfused (~1.5 ml/min) with a saline solution containing 90 mM NaCl, 3 mM KCl, 0.82 mM $MgCl_2$, 0.74 mM $CaCl_2$, 10 mM HEPES-Tris, pH 7.6. After microelectrode impalement, a membrane potential stabilization period of 1–10 min was observed. Oocytes whose membrane potential was less negative than −35 mV were discarded. The membrane potential was then held at −50 mV, following which a voltage range from +75 mV to −175 mV was covered in 25-mV steps. The oocyte membrane potential was stepped to the new levels for 250-ms intervals, and traces were analyzed by averaging the signal in a window of 50 ms positioned after the decay of capacitive transient currents. The measurements are generally taken in the absence and in the presence of a particular substrate, and the substrate-specific current is determined by subtraction of one current from the other. When the concentration of NaCl was diminished, it was isotonically replaced with *N*-methyl-D-glucamine chloride. All of the steady-state and presteady-state current experiments were performed at room temperature (24 °C).

Measurement and Analysis of Presteady-state Currents—For the recording of presteady-state currents, the voltage pulse duration was reduced to 50 ms, and the sampling rate was increased to 0.1 ms/point. The membrane potential was stepped from +50 mV to −175 mV in 25-mV increments from a holding potential of −50 mV. The currents measured in the presence of 0.5 mM phlorizin were subtracted (point by point) from the total currents measured in a saline solution ($[Na^+]_{out}$ = 30 mM). The displaced charge (Q) was obtained by integrating the transient portion of the presteady-state currents, and the Q *versus* V_m curve was fitted to the following Boltzmann equation,

$$Q = \frac{Q_{dep} - Q_{hyp}}{(1 + e^{\left[\frac{(V_m - V_{0.5})zF}{RT}\right]})} + Q_{hyp} \qquad \text{(Eq. 1)}$$

where Q_{hyp} and Q_{dep} are the charges transferred at hyperpolarizing and depolarizing V_m, z is the valence of the mobile charge, $V_{0.5}$ is the V_m at which half of the charge is transferred, and F, R, and T are the usual constants. Fitting was done using the Levenberg-Marquardt algorithm (Origin 6.1, OriginLab Corp., Northampton, MA).

RESULTS

Expression of rkST1 in *Xenopus* oocytes was impeded by a lethal effect of the protein on the host cells. Injection of 46 nl of rkST1 mRNA at a concentration of 0.25, 0.5, or 1.0 μg/μl resulted in the death of all oocytes by the third day following injection (as judged either visibly or by membrane potential measurement) when incubated in serum-free Barth's solution; injection of 0.1 μg/μl mRNA caused about half of the oocytes to die. The mortality rate was reduced by inclusion of 5% horse serum in the incubation medium (26), which resulted in survival of all oocytes injected with 0.1 μg/μl mRNA as well as half of those injected with 0.25 μg/μl mRNA. Inclusion of either 500 μM phlorizin or 5 mM MI in the Barth's solution did not affect the survival rate. Subsequent experiments were performed after injecting oocytes with 46 nl of 0.1 μg/μl mRNA and maintaining the oocytes in Barth's solution containing 5% serum.

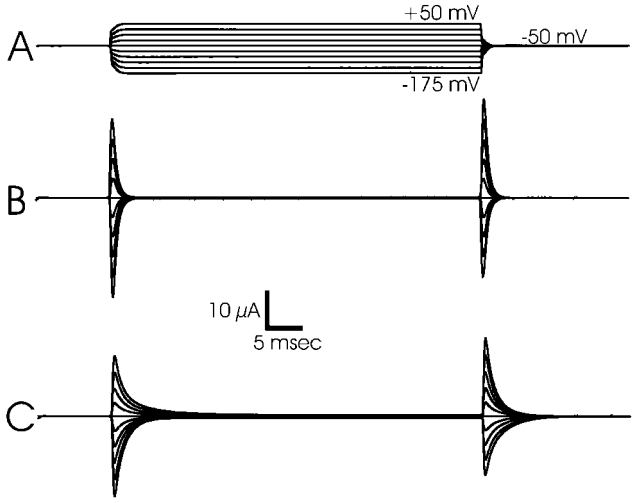

FIG. 1. **Presteady-state current recordings.** The oocytes were held at a membrane potential of −50 mV, which was then stepped to levels between +50 mV and −175 mV for 50-ms periods. A series of recordings of the membrane potential from a typical oocyte undergoing this voltage clamp protocol is shown (*A*). The total currents across the oocyte membrane were measured and are displayed for typical oocytes that had been injected with water (*B*) or with rkST1 mRNA (*C*). NaCl was present at 90 mM in this series of experiments, but no MI was present.

The initial indication that the rkST1 protein was expressed in the oocyte plasma membrane was provided by the presteady-state currents created by briefly stepping the membrane potential of oocytes from the holding potential of −50 mV to intermediate levels between −175 mV and +50 mV. As seen in Fig. 1, control (water-injected) oocytes display a capacitive current that decays within 1.5–2.5 ms. Oocytes injected with rkST1 mRNA display an additional current that continues to decay well after the membrane potential has stabilized at a new level. This is similar to the presteady-state currents observed with other cotransporter proteins (28–30), confirming that an exogenous protein has been expressed at the plasma membrane. Although not all membrane proteins are likely to be characterized by presteady-state currents when expressed *in ovo*, this phenomenon holds true for all of the SLC5 family members that have been examined.

The oocytes expressing rkST1 were then superfused with several substrates, including glucose and MI, while the oocyte membrane potential was held at −50 mV. A large, reversible, steady-state inward current was associated with exposure to 1 mM MI (Fig. 2), whereas a much smaller current was associated with exposure to 1 mM glucose. Superfusion with 1 mM α-methylglucose, a specific substrate for SGLT1, did not cause any current flow through rkST1, whereas a small inward current was blocked by application of 0.5 mM phlorizin, similar to substrate-independent currents seen with other cotransporters (31, 32). Because the protein evinced the greatest currents following exposure to MI, we have named it SMIT2, and we suggest that the first SMIT protein be renamed SMIT1, with the consent of the original authors.[2] A large current was also observed with superfusion of D-*chiro*-inositol, but only a very small current was seen with L-*chiro*-inositol superfusion. None of these currents were seen in the absence of sodium.

To better characterize the substrate specificity of this transporter, we superfused SMIT2-expressing oocytes with 50 mM of either MI or a variety of sugars to be able to compare SMIT2 transport with results similarly obtained by others with SGLT1

[2] J. S. Handler, personal communication.

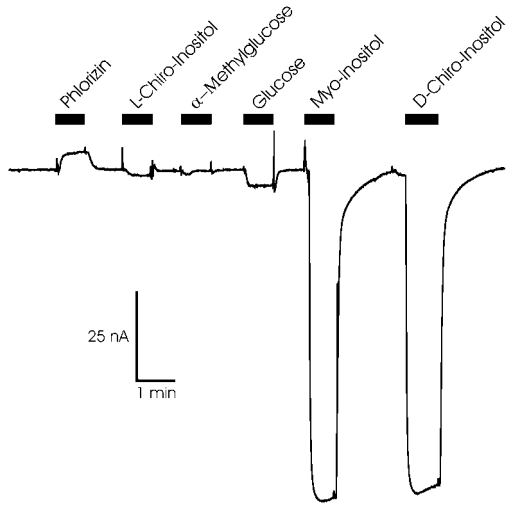

FIG. 2. **Substrate transport through the rkST1 (SMIT2) protein.** The oocyte was clamped at −50 mV and superfused with a saline solution containing 90 mM NaCl. The substrates were superfused at a concentration of 1 mM; phlorizin was superfused at a concentration of 500 μM.

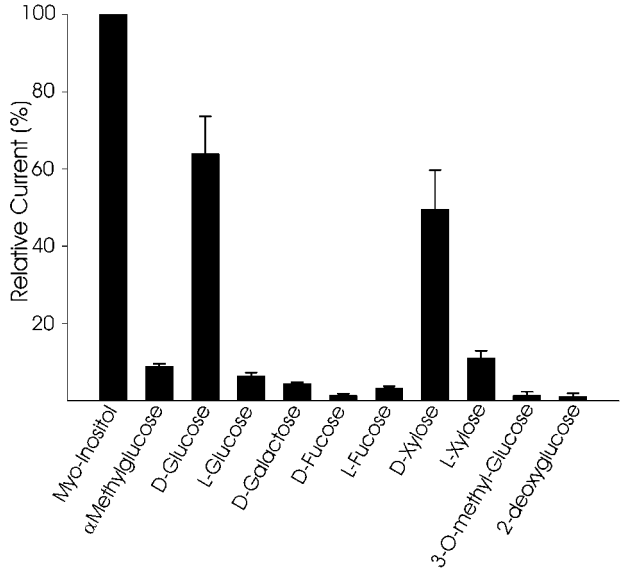

FIG. 3. **Sugar selectivity of SMIT2.** The oocytes expressing SMIT2 were exposed to 50 mM of each substrate in a modified saline solution (containing 65 mM NaCl). The sugar-induced currents were measured at a holding potential of −50 mV. Each sugar-dependent current was expressed as a percentage of the current induced when that same oocyte was superfused with 50 mM MI. The data represent the averages and S.E. for six oocytes, taken from a total of three donor animals. The average current observed with SMIT2-expressing oocytes in 50 mM MI was −285 ± 150 nA.

and SMIT1 (28) (Fig. 3). The solutions contained 65 mM NaCl, and tonicity was maintained by the inclusion of 50 mM mannitol in the absence of MI or other sugars (mannitol did not induce measurable currents through SMIT2). To eliminate the variability caused by the different levels of SMIT2 expression in individual oocytes, the results from each oocyte are expressed as percentages of the current observed when 50 mM MI was applied to the same oocyte. There are several intriguing differences between the substrate specificities of SMIT1 and SMIT2. The most obvious is that SMIT2 has a greater affinity for D-glucose than does SMIT1, because 50 mM D-glucose produces a current through SMIT2 that is over half the size of the current seen with 50 mM MI but less than 25% of the MI current is seen when 50 mM D-glucose is applied to SMIT1 (28).

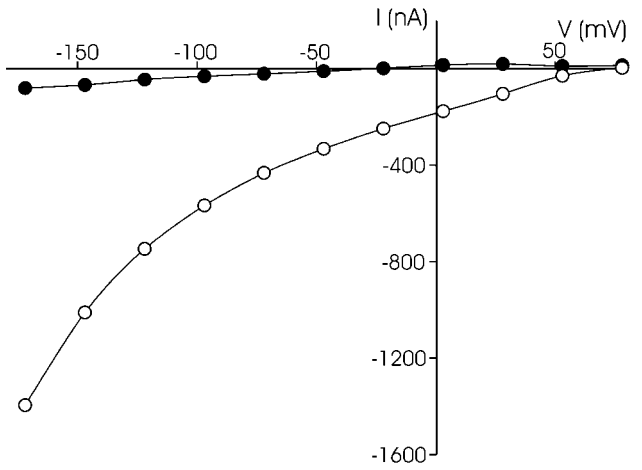

FIG. 4. **Current-voltage relationship for SMIT2.** The currents in a typical SMIT2-expressing oocyte, caused by the addition of MI (○), were obtained by subtracting the currents measured at −50 mV in the presence of 500 μM MI from currents measured in the absence of MI. The *black circles* display the phlorizin-inhibitable sodium leak currents obtained by subtracting currents measured in the presence of 500 μM phlorizin from currents measured in the absence of phlorizin (all in the absence of MI).

SMIT2 exhibits stereospecificity, transporting D-glucose and D-xylose but not their L-stereoisomers. None of the other sugars tested with SMIT2 induced significant currents. SMIT1, in contrast, transports L-fucose and L-xylose (but not their D-isomers) and does not distinguish between D- and L-glucose. Neither does SMIT1 distinguish between α-methylglucose and D-glucose, whereas SMIT2 displays far more transport of D-glucose than of α-methylglucose at 50 mM substrate. Although L-fucose has been shown to inhibit SMIT1 (33), we found no inhibition of the SMIT2 current associated with 100 μM MI when 5 mM L-fucose was added to the MI (data not shown).

The current-voltage (I-V) relationship of SMIT2 was examined by subtracting the currents measured in the absence of MI from those observed in the presence of 1 mM MI; the difference between them represents the substrate-dependent current passing through SMIT2. No MI-dependent current was observed in control (water-injected) oocytes, whereas superfusion of MI causes a large inward current through SMIT2, which increased in magnitude as the membrane potential grew more negative (Fig. 4). The current showed no evidence of having attained a maximal level at the most negative potential used (−175 mV), which is similar to the I-V curve seen with SMIT1 expression but unlike the shape of the I-V curve for SGLT1 (28). The currents for the phlorizin-sensitive sodium leak associated with SMIT2 were also examined at different membrane potentials (Fig. 4). The magnitude of this current at highly negative potentials is on the order of 5% of the substrate-dependent current, similar to the size of the SGLT1 leak current (31). The outward sodium leak currents at positive potentials are negligible, unlike those seen with SGLT1 (31).

We have also examined the voltage sensitivity of the kinetic constants of SMIT2. The K_m value for MI remains quite constant, near 120 μM, over the voltage range of −175 mV to −25 mV (Fig. 5*A*); this is approximately twice as high as the K_m for SMIT1 (which is also relatively voltage-independent). The kinetic parameters at membrane potentials more positive than −25 mV were found to be unreliable because of a vanishingly small steady-state MI-dependent current. Not surprisingly, the calculated I_{max} values found while varying MI or sodium concentrations both comprise curves that conform to the I-V curve seen in Fig. 4 at the relatively high MI concentration of 1 mM with 90 mM sodium (Fig. 5*B*). The K_m for sodium was lowest at

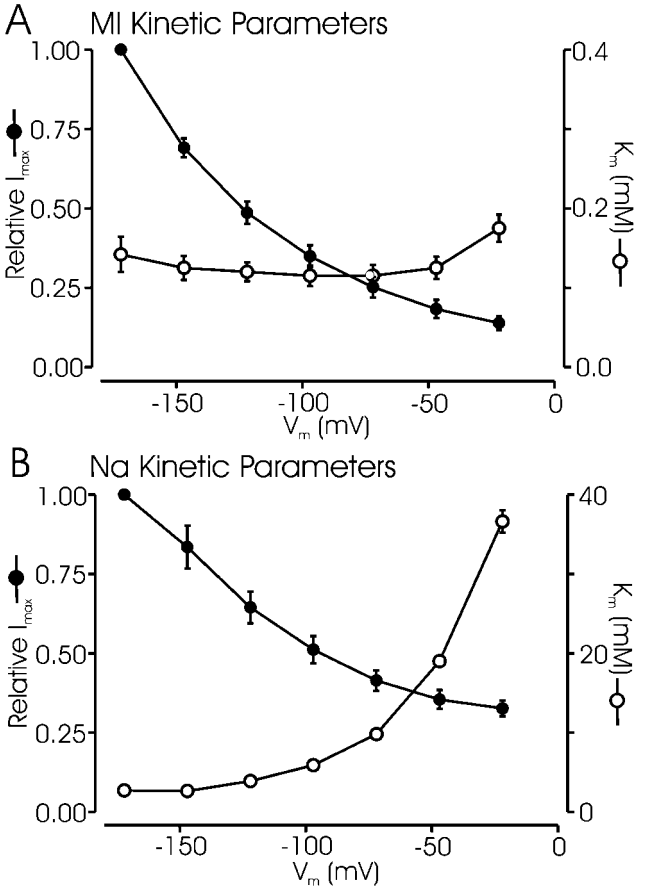

FIG. 5. **Substrate and voltage dependence of SMIT2 activity.** SMIT2-expressing oocytes were exposed to different concentrations of MI or sodium and steady-state currents were measured in each solution at different membrane potentials. *A*, the MI-dependent currents were fitted to the Michaelis-Menten equation. The I_{max} calculated at each membrane potential for each oocyte was divided by the I_{max} calculated at −175 mV, and the means and S.E. were derived from these normalized currents to eliminate interoocyte variability in SMIT2 expression levels. n = 10, sodium = 90 mM. *B*, MI-dependent currents were obtained in solutions of varying sodium concentration and were fit to the Michaelis-Menten equation. I_{max} values were calculated in the same fashion as described above. n = 5, MI = 1 mM.

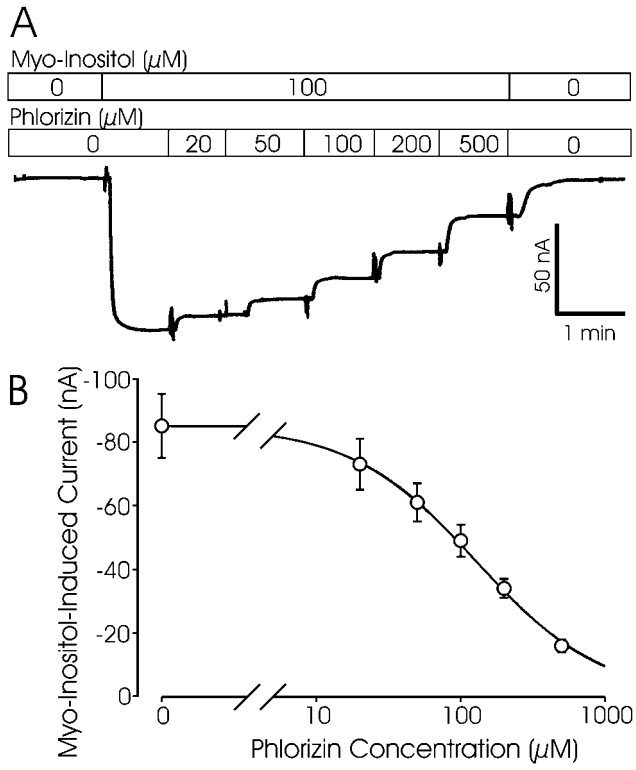

FIG. 6. **Phlorizin inhibition of MI current.** *A*, a typical SMIT2-expressing oocyte demonstrated inward currents when exposed to MI that were gradually inhibited as increasing amounts of phlorizin were added to the superfusion medium. *B*, currents measured in the presence of different phlorizin concentrations were obtained from nine oocytes. The *line* represents a fit of all of the data by nonlinear regression to the equation for competitive inhibition. The *symbols* and *error bars* represent the means and S.E. for the currents measured at each phlorizin concentration.

the most negative potentials, rising quickly when the membrane potential approached zero. One noteworthy difference between the sodium affinities of the two SMIT proteins is that the SMIT2 K_m reached an extremely low value (2.7 mM) at −175 mV, whereas the K_m values seen with SMIT1 appears to attain a lower limit near 40 mM (28). The sodium K_m value for SGLT1, by comparison, presents a voltage dependence that appears very similar to that seen with SMIT2 (31). At −50 mV, our data was fit to the Hill equation and produced a Hill coefficient of 1.4 (data not shown), indicating significant cooperativity, which suggests a stoichiometry greater than 1:1. It should also be mentioned that, at −50 mV, the K_m for D-*chiro*-inositol is 130 ± 10 μM, and the I_{max} is identical to that seen with MI (Fig. 2). The K_m for D-glucose is ~30 mM at −50 mV, whereas the I_{max} appears identical to that determined with MI.

We turned to measurements of the reversal potential to further pursue the question of stoichiometry (34). In the presence of 100 μM MI, varying concentrations of phlorizin were used while recording the MI-dependent current (Fig. 6). As analyzed by competitive inhibition, a K_i of 76 μM was obtained. Analysis of the phlorizin-sensitive current showed very little outward current, and even conditions of preloading with MI or with lower external [Na] failed to induce a reliable reversal potential. Consequently, we were unable to use the reversal potential of the Na$^+$/MI current to estimate the stoichiometry of the cotransport protein, as had been done for SGLT1 (34).

The presteady-state currents associated with SMIT2 expression in *Xenopus* oocytes were examined by subtracting the currents measured in the presence of 0.5 mM phlorizin from those measured in the absence of phlorizin (Fig. 7). No MI was present, and the sodium concentration was reduced to 30 mM to bring the $V_{0.5}$ toward more positive potentials. The presteady-state currents are present whenever the potential is clamped to a new value; there are also some steady-state currents caused by the substrate-independent current that passes through SMIT2. Integration of the presteady-state current produced a transferred charge *versus* potential curve, which can be fitted with a Boltzmann relation described by a Q_{max} value of 11.7 ± 0.5 nC, a $V_{0.5}$ of −11 ± 3 mV, and a z value of 1.21 ± 0.05. Given these z and Q_{max} values, the number of transporters/oocyte can be calculated at 5.8×10^{10}. Assuming a I_{MI} of 200 nA at −50 mV, the turnover rate must be either 23 s^{-1} (assuming a Na$^+$:MI stoichiometry of 1:1) or 11.5 s^{-1} (assuming a Na$^+$:MI stoichiometry of 2:1).

DISCUSSION

The SMIT2 cDNA was first cloned in 1994 by Hitomi and Tsukagoshi (4) using PCR with degenerate primers against a conserved sequence motif. Sequence analysis and comparison within the SLC5 family suggested a 12–14 TMS protein with 49 and 43% sequence identity to SGLT1 and SMIT1, respectively. SMIT2 RNA had been detected in brain, kidney, heart, skeletal muscle, spleen, liver, placenta, lung, leukocytes, and neurons

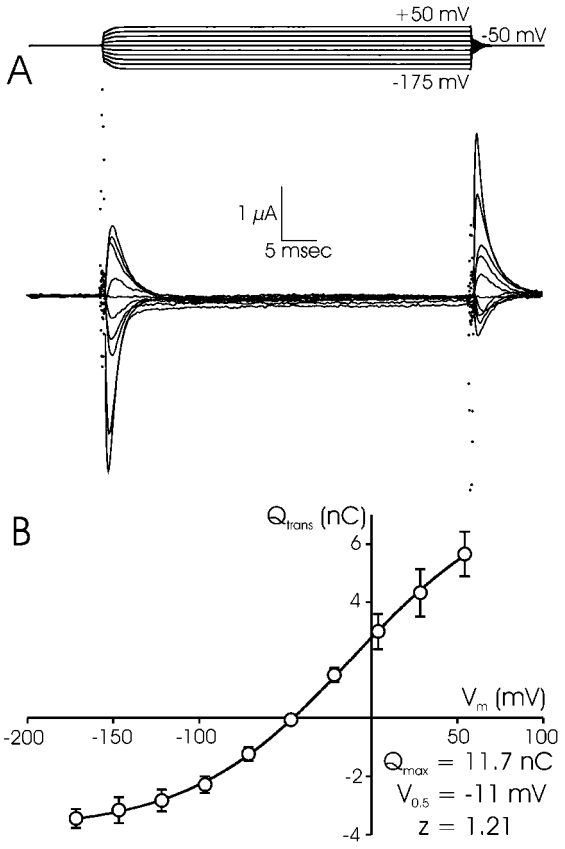

FIG. 7. **Presteady-state currents of SMIT2-expressing oocytes.** *A*, the membrane potential was stepped from the holding potential (−50 mV) to potentials at 25 mV intervals between −175 and 50 mV for 50-ms periods. The presteady-state currents were obtained by subtracting the currents measured in the presence of 0.5 mM phlorizin from those measured in the absence of phlorizin, with data filtered at 1 kHz. Both solutions contained 30 mM Na^+. The first 0.8 ms following the change in potential has been rendered as *dots* to better visualize the presteady-state currents recorded once 90% of the voltage step has been completed. *B*, the charge transferred during the presteady-state currents was calculated by integrating the phlorizin sensitive current and fitted to Equation 1. $Q_{max} = Q_{dep} - Q_{hyp} = 11.3$ nC, $V_{0.5} = -11$ mV, and $z = 1.21$. The *error bars* represent the S.E. ($n = 5$ oocytes).

(4, 35, 36), but the function of the protein had never been established.

Identifying the function of an orphan cotransporter in *Xenopus* oocytes can be greatly aided by first establishing that the protein is actually expressed at the cell membrane. A number of other orphan proteins have not displayed significant currents after exposure to a battery of possible substrates, and there are examples where this has occurred because the protein was not expressed at the cell surface during heterologous expression in oocytes (23). The presteady-state currents displayed by SMIT2 are large and long-lived, enabling us to easily observe them and giving us confidence that the orphan protein was correctly expressed at the cell surface.

SMIT2, when expressed in oocytes, transports MI with a K_m (120 μM) closely corresponding to the 70 μM human plasma concentration of MI (14) and well below the 470 μM concentration reported for cerebrospinal fluid (37) and has a substantial I_{max} that compares well with other sodium-coupled cotransporters. Furthermore, the K_m for glucose is well above normal serum glucose levels. It seems clear that MI is the physiological substrate for the protein; although D-*chiro*-inositol is transported as readily as MI, the average serum level of D-*chiro*-inositol is less than 100 nM (38), and thus D-*chiro*-inositol transport represents a minor physiological role for SMIT2. It should be noted that there has been one previous publication suggesting the names SMIT1, SMIT2, and SMIT3 for three alternate transcripts from the SLC5A3 gene (39); we suggest that these be named SMIT1a, SMIT1b, and SMIT1c, in which we have the consent of the authors of that work.[3]

SMIT2 displays properties that are similar to those of the best studied sodium-coupled transporter, SGLT1. Like SGLT1, SMIT2 is phlorizin-sensitive, has a sodium leak and presents presteady-state currents; the sodium activation is slightly cooperative, suggesting a stoichiometry of 2 sodium for 1 MI molecule; and its estimated turnover rate is of the order of 10. On the other hand, it also presents very noticeable differences *versus* SGLT1. The I-V relationship does not saturate at negative membrane potentials, indicating that, as seems to be the case for SMIT1, a voltage-dependent step remains rate-limiting throughout the voltage range studied. The sugar affinity remains approximately constant from −25 to −175 mV. One of the most striking differences between SMIT1 and SMIT2 is that SMIT2 displays specificity for the D-stereoisomers of the most prevalent biological substrates (*chiro*-inositol and glucose), whereas SMIT1 has no such preference. These differences in substrate selectivity may be useful for delineating the functional differences between the two proteins *in vivo*, where they are both expressed in kidney and brain (2, 36). The lack of transport of galactose by SMIT2 conforms to a motif proposed recently in which proteins of the SLC5 family that have a threonine at the position homologous to residue 460 in human SGLT1 are able to transport galactose, whereas the other SLC5 proteins (such as SMIT2) do not transport galactose (40).

A recent publication described the human SMIT2 cDNA sequence and examined the distribution of SMIT2 expression by Northern blot analysis (41). SMIT2 appears to be quite widely distributed, although it is not present in small intestine and some other tissues. In particular, SMIT2 is well expressed in brain, heart, muscle, kidney, and liver. In other work, SMIT1 and SMIT2 have been detected in neurons, both in glial cells and in astrocytes (35). Because the control of MI uptake into the cells of the central nervous system has been suggested to be related to the control of a variety of psychiatric illnesses (42–44), a better understanding of the roles for SMIT1 and SMIT2 in brain may aid the investigation of these maladies. The group that identified the human homologue of SMIT2 has also examined the possibility of a link between this gene and an inherited disorder of infantile convulsions that has been mapped to this region of the genome but found no link between carriers of the disease and specific polymorphisms within the cDNA.

SMIT2 appears to be similar to a cotransporter from HepG2 cells that was previously shown to transport MI and D-*chiro*-inositol with similar affinities (18). As was seen for SMIT2, the novel transporter described in these cell cultures displayed similar K_m values for the two inositols and exhibited competition from D-glucose but not from L-glucose. The same cell line also appeared to express SMIT1, indicating that the two proteins can coexist in the same cells. No information is yet available regarding the distribution of the two cotransporters between the different plasma membrane domains in these polarized cells. Lack of inhibition of SMIT2 by L-fucose suggests that SMIT2 is not involved in several transport phenomena involving competition between L-fucose and MI, including diabetic neuropathy (45). It should be noted, however, that SMIT2 has a greater affinity for glucose than does SMIT1 and is thus more likely to be affected by increased glucose levels during untreated diabetes.

The SMIT2 peptide sequence is most closely related to the

[3] M. J. Stevens, personal communication.

Xenopus SGLT1-like protein (xSGLT1L). They are 67% identical, whereas SMIT2 is only 43% identical to SMIT1 and 49% identical to SGLT1. It is difficult to firmly establish whether SMIT2 and xSGLT1L represent true orthologues; by comparison there is 75% identity between the human SGLT1 and SGLT3 peptide sequences. Functional comparison of the two proteins is also ambiguous; although xSGLT1L transports both MI and glucose, its affinity for MI is half that of SMIT2, whereas xSGLT1L has a lower K_m for glucose (6.3 mM *versus* ~30 mM for SMIT2). Furthermore, the K_i for phlorizin interaction with xSGLT1L is 6.3 μM, whereas it inhibits SMIT2 with a K_i of 76 μM. The current-voltage relationships for the two proteins are also somewhat different because xSGLT1L, like SGLT1, appears to reach a plateau in the current obtained as the potential becomes quite negative. SMIT2, on the other hand, generates increasingly large currents as the potential becomes more negative, similar to that seen with SMIT1. SMIT2 also displays sodium leak currents (substrate-independent, phlorizin-inhibitable), whereas xSGLT1L has no sodium leak currents. The strongest evidence that SMIT2 and xSGLT1L represent different proteins is that the distribution of SMIT2 is primarily in the kidney, liver, heart, and brain (but not intestine), whereas xSGLT1L is found primarily in the intestine and kidney (6, 46). It seems likely that the two proteins are orthologous but that they serve somewhat different roles in mammals and amphibians.

There have been a number of reports that indicate multiple MI transport activities in different tissues, and the identification of SMIT2 may illuminate some of these situations. Precise location of SMIT2 *in vivo* will require immunohistochemical techniques. The substrate specificity of SMIT2 does match that of a transporter that has been observed in renal proximal tubule apical membranes (47). Because the RNAs coding for SMIT1, SMIT2, and HMIT appear to be absent from small intestine (2, 23, 41), the identification of the intestinal MI transporter remains to be determined. The presence of three distinct MI cotransporters in brain tissues complicates the issue of MI metabolism in the central nervous system, which has gained prominence with the recent identification of MI depletion as the mechanism of action of three drugs commonly used to treat bipolar affective disorder (48).

REFERENCES

1. Hediger, M. A., Coady, M. J., Ikeda, T. S., and Wright, E. M. (1987) *Nature* **330,** 379–381
2. Kwon, H. M., Yamauchi, A., Uchida, S., Preston, A. S., Garcia-Perez, A., Burg, M. B., and Handler, J. S. (1992) *J. Biol. Chem.* **267,** 6297–6301
3. Wright, E. M. (2001) *Am. J. Physiol.* **280,** F10–F18
4. Hitomi, K., and Tsukagoshi, N. (1994) *Biochim. Biophys. Acta* **1190,** 469–472
5. Pajor, A. M. (1994) *Biochim. Biophys. Acta* **1194,** 349–351
6. Nagata, K., Hori, N., Sato, K., Ohta, K., Tanaka, H., and Hiji, Y. (1999) *Am. J. Physiol.* **276,** G1251–G1259
7. Downes, C. P., and Macphee, C. H. (1990) *Eur. J. Biochem.* **193,** 1–18
8. Toker, A., and Cantley, L. C. (1997) *Nature* **387,** 673–676
9. Nakanishi, T., Balaban, R. S., and Burg, M. B. (1988) *Am. J. Physiol.* **255,** C181–C191
10. Wiese, T. J., Dunlap, J. A., Conner, C. E., Grzybowski, J. A., Lowe, W. L., and Yorek, M. A. (1996) *Am. J. Physiol.* **270,** C990–C997
11. Trachtman, H. (1992) *Pediatr. Nephrol.* **6,** 104–112
12. Ashizawa, N., Yoshida, M., and Aotsuka, T. (2000) *J. Biochem. Biophys. Methods* **44,** 89–94
13. MacGregor, L. C., and Matschinsky, F. M. (1984) *Anal. Biochem.* **141,** 382–389
14. Dolhofer, R., and Wieland, O. H. (1987) *J. Clin. Chem. Clin. Biochem.* **25,** 733–736
15. Schmolke, M., Bornemann, A., and Guder, W. G. (1990) *Biol. Chem. Hoppe-Seyler* **371,** 909–916
16. Nakanishi, T., Turner, R. J., and Burg, M. B. (1989) *Proc. Natl. Acad. Sci. U. S. A.* **86,** 6002–6006
17. Novak, J. E., Turner, R. S., Agranoff, B. W., and Fisher, S. K. (1999) *J. Neurochem.* **72,** 1431–1440
18. Ostlund, R. E., Jr., Seemayer, R., Gupta, S., Kimmel, R., Ostlund, E. L., and Sherman, W. R. (1996) *J. Biol. Chem.* **271,** 10073–10078
19. Cammarata, P. R., Chen, H. Q., Yang, J., and Yorio, T. (1992) *Invest. Ophthalmol. Vis. Sci.* **33,** 3572–3580
20. Sigal, S. H., Yandrasitz, J. R., and Berry, G. T. (1993) *Metabolism* **42,** 395–401
21. Noh, S. J., Kim, M. J., Shim, S., and Han, J. K. (1998) *J. Cell. Physiol.* **176,** 412–423
22. Warfield, A., Hwang, S. M., and Segal, S. (1978) *J. Neurochem.* **31,** 957–960
23. Uldry, M., Ibberson, M., Horisberger, J. D., Chatton, J. Y., Riederer, B. M., and Thorens, B. (2001) *EMBO J.* **20,** 4467–4477
24. Kaluz, S., Kolble, K., and Reid, K. B. (1992) *Nucleic Acids Res.* **20,** 4369–4370
25. Pokrovskaya, I. D., and Gurevich, V. V. (1994) *Anal. Biochem.* **220,** 420–423
26. Quick, M. W., Naeve, J., Davidson, N., and Lester, H. A. (1992) *BioTechniques* **13,** 357–361
27. Coady, M. J., Jalal, F., Chen, X., Lemay, G., Berteloot, A., and Lapointe, J. Y. (1994) *FEBS Lett.* **356,** 174–178
28. Hager, K., Hazama, A., Kwon, H. M., Loo, D. D., Handler, J. S., and Wright, E. M. (1995) *J. Membr. Biol.* **143,** 103–113
29. Mackenzie, B., Loo, D. D., Panayotova-Heiermann, M., and Wright, E. M. (1996) *J. Biol. Chem.* **271,** 32678–32683
30. Forster, I. C., Wagner, C. A., Busch, A. E., Lang, F., Biber, J., Hernando, N., Murer, H., and Werner, A. (1997) *J. Membr. Biol.* **160,** 9–25
31. Umbach, J. A., Coady, M. J., and Wright, E. M. (1990) *Biophys. J.* **57,** 1217–1224
32. Forster, I., Hernando, N., Biber, J., and Murer, H. (1998) *J. Gen. Physiol* **112,** 1–18
33. Yorek, M. A., Stefani, M. R., Dunlap, J. A., Ro, K. S., and Davidson, E. P. (1991) *Diabetes* **40,** 1016–1023
34. Chen, X. Z., Coady, M. J., Jackson, F., Berteloot, A., and Lapointe, J. Y. (1995) *Biophys. J.* **69,** 2405–2414
35. Poppe, R., Karbach, U., Gambaryan, S., Wiesinger, H., Lutzenburg, M., Kraemer, M., Witte, O. W., and Koepsell, H. (1997) *J. Neurochem.* **69,** 84–94
36. Barak, Y., Levine, J., Glasman, A., Elizur, A., and Belmaker, R. H. (1996) *Prog. Neuropsychopharmacol. Biol. Psychiatry* **20,** 729–735
37. Spector, R., and Lorenzo, A. V. (1975) *Am. J. Physiol.* **228,** 1510–1518
38. Ostlund, R. E., Jr., McGill, J. B., Herskowitz, I., Kipnis, D. M., Santiago, J. V., and Sherman, W. R. (1993) *Proc. Natl. Acad. Sci. U. S. A.* **90,** 9988–9992
39. Porcellati, F., Hosaka, Y., Hlaing, T., Togawa, M., Larkin, D. D., Karihaloo, A., Stevens, M. J., Killen, P. D., and Greene, D. A. (1999) *Am. J. Physiol.* **276,** C1325–C1337
40. Diez-Sampedro, A., Wright, E. M., and Hirayama, B. A. (2001) *J. Biol. Chem.* **276,** 49188–49194
41. Roll, P., Massacrier, A., Pereira, S., Robaglia-Schlupp, A., Cau, P., and Szepetowski, P. (2002) *Gene* (*Amst.*) **285,** 141–148
42. Benjamin, J., Levine, J., Fux, M., Aviv, A., Levy, D., and Belmaker, R. H. (1995) *Am. J. Psychiatry* **152,** 1084–1086
43. Fux, M., Levine, J., Aviv, A., and Belmaker, R. H. (1996) *Am. J. Psychiatry* **153,** 1219–1221
44. Levine, J., Barak, Y., Gonzalves, M., Szor, H., Elizur, A., Kofman, O., and Belmaker, R. H. (1995) *Am. J. Psychiatry* **152,** 792–794
45. Sima, A. A., Dunlap, J. A., Davidson, E. P., Wiese, T. J., Lightle, R. L., Greene, D. A., and Yorek, M. A. (1997) *Diabetes* **46,** 301–306
46. Eid, S. R., Terrettaz, A., Nagata, K., and Brändli, A. W. (2002) *Int. J. Dev. Biol.* **46,** 177–184
47. Silbernagl, S., Völker, K., and Dantzler, W. H. (2001) *I.U.P.S. XXXIVth International Congress*, Abstract number 853, CD-ROM for the 2001 meeting (iups.mcw.edu)
48. Williams, R. S., Cheng, L., Mudge, A. W., and Harwood, A. J. (2002) *Nature* **417,** 292–295

Identification of a Novel Na^+/*myo*-Inositol Cotransporter

Michael J. Coady, Bernadette Wallendorff, Dominique G. Gagnon and Jean-Yves Lapointe

J. Biol. Chem. 2002, 277:35219-35224.
doi: 10.1074/jbc.M204321200 originally published online July 19, 2002
